IDRiM (2025) 15 (2) **ISSN: 2185-8322**
DOI10.5595/001c.144969

Journal of Integrated Disaster Risk Management

Regular Article

Fire Risk Assessment in Informal Refugee Settlements: A Case Study of the Rohingya Refugee Camps, Cox's Bazar

Md. Syadur Rahaman[1*] and Nurun Nahar[2]

Received: 14/11/2024 / Accepted: 17/07/2025 / Published online: 16/10/2025

Abstract Fires pose severe threats to informal settlements, notably in refugee camps within developing nations. To devise an effective fire risk reduction strategy, a comprehensive, indicator-based risk assessment using GIS and AHP, methods commonly applied in forest fire studies, was conducted to evaluate fire hazards at the shelter level in the Rohingya Refugee Camps. The assessment incorporated 12 indicators from prior reports and available data to measure hazard exposure, vulnerability, and capacity. The risk score, derived from these components, ranged from 0 to 1 and was categorized using the INFORM risk methodology into five levels: Very Low, Low, Moderate, High, and Very High. Results indicated that 44.1% of the settlements face very high risk, 32.9% are at high risk, 17.2% are at moderate risk, and the remaining areas are at low to very low risk. Notably, Camps 1E, 1W, 2W, 3, 7, 9, 10, 11, 15, and NRC showed the highest proportion of high-risk shelters, whereas Camps 4Ex, 20, 20Ex, 21, 25, and 27 were identified as lower risk zones. These findings provide critical insights for targeted disaster management strategies and effective resource allocation by humanitarian agencies, enhancing fire risk mitigation in the camp and similar contexts.

Keywords: informal settlements, AHP, Fire Hazard Risk Index, refugee camp, GIS

1. INTRODUCTION

The recent years, the world has witnessed an alarming surge in the number of forcibly displaced individuals due to climate change, disaster, persecution, conflict, violence, and human rights violations. A UNHCR study reports that by the end of 2022, approximately 108.4

[1] Institute of Water and Flood and Management (IWFM), Bangladesh University of Engineering and Technology, Bangladesh
[2] Computer Science and Engineering, Dhaka International University, Bangladesh
* Corresponding author email: syadur.du.2013@gmail.com

million people were forcibly displaced, seeking safety and refuge worldwide, with 76% of these individuals hosted in low- and middle-income countries. (UNHCR, 2023b, 2023a). Notably, Bangladesh has hosted nearly one million refugees from Myanmar's Rakhine State since 2017 (UNHCR, 2024b). In response to this unprecedented crisis, UNHCR's 2024 appeal for $10.622 billion to support 130.8 million forcibly displaced and stateless individuals (UNHCR, 2024a). However, the international response has been underwhelming, likely due to competing priorities and the frequent occurrence of the crisis in the wealthier nations (UNHCR, 2024a). The number of refugees is increasing day by day, and the life of refugees is becoming harder. With a diverse range of conflicts, change came with serious threats to humans where no one could be safe. Therefore, a multidimensional crisis develops against the solution of the refugees (UNHCR, 2023a).

Disasters have significantly contributed to disparities in both human well-being and property across the globe. The latest Global Assessment Report highlights a noteworthy trend: developing and least developed nations bear the brunt of more devastating events compared to their developed counterparts (UNDRR, 2022a). A prime example of this vulnerability is evident in Bangladesh, a country prone to a range of natural and human-caused hazards, including floods, cyclones, landslides, fires, building collapses, salinity intrusion, and droughts (Mukherjee et al., 2023; Parvin et al., 2022). These disasters do not affect all regions of the country equally. The National Risk Atlas and INFORM Sub-National Risk Index pinpoint Cox's Bazar as one of the most susceptible districts, particularly prone to cyclones, fires, landslides, and salinity issues (MoDMR, 2021; UNDRR, 2022). Adding to this vulnerability is the fact that Cox's Bazar is home to over one million forcibly displaced refugees from Myanmar, Rohingya. Their circumstances are even direr due to inadequate living conditions and limited access to essential infrastructure and resources.

After the massive influx in 2017, we have seen several events take place in the Rohingya refugee camp. Both natural and anthropogenic hazards are present in the camp. Fire is a common human-induced incident that happens in the Rohingya refugee camp and is the most devastating disaster. Last few years we have seen some devastating fire incidents in the Rohingya refugee camps at an increasing rate. The daily incident report database shows that in 2021, there were only twelve fire incidents, but in 2022, there were 100 incidents that took place in the camps (IOM, 2023a). This is due to the overcrowded and squalid conditions in the camps, as well as the use of flammable materials for cooking and heating. The most recent fire incident occurred on March 5, 2023, in Camp 11 of Cox's Bazar refugee camp destroying over 2,800 shelters and leaving 15,000 refugees homeless (IOM, 2023b).

The worldwide considerable number of studies conducted to explore the causes and fire in forests also try to identify the nature of spread, the magnitude of the fire (Cicione et al., 2021; Flores Quiroz et al., 2021; Guevara Arce et al., 2021; Hu et al., 2022; Kazerooni et al., 2016; Morrissey & Taylor, 2006; Quiroz et al., 2021). Very limited study has been done to explore the risk scenarios of informal settlements (IS) like Rohingya refugee camps. The factors that contributed to the rapid spread of the fire in Cox's Bazar refugee camp include the highly combustible nature of the homes in the camp and the dense nature of the settlements (Flores Quiroz et al., 2023). These factors significantly affected the fire spread rates. Additionally, the

presence of multiple fires occurring at the same time could be attributed to spot ignitions caused by firebrands or hot metal fragments being carried by the wind. The main challenges faced in terms of evacuation routes and resources in refugee camps during large-scale fire incidents include (if) Insufficient exit routes; (ii) Unfamiliarity with the area; (iii) Limited resources and infrastructure (iv) Communication barriers; (v) High population density; (vi) Structural vulnerabilities; (vii) Security measures and (viii) Limited fire safety education (Flores Quiroz et al., 2023). Additionally, the existing firefighting techniques are not effectively equipped to manage the specific challenges posed by the construction of new structures within the camp areas. These factors contribute significantly to the increased vulnerability to fires in the camps.

However, a notable gap remains in our comprehension of the intricate dynamics of fire hazards and their profound impact on refugee camps, particularly within the context of a multi-hazard vulnerability and risk scenario present in the Camps. The current research endeavor seeks to delve into the multifaceted aspects of fire risks within the Rohingya refugee camp. This research aims to develop the individual shelter-level fire hazard risk index using the Analytical Hierarchy Process (AHP). By doing so, we aim to contribute to a deeper understanding of these dynamics and subsequently inform more effective fire disaster risk management strategies.

2. STUDY AREA

The research site encompasses the Rohingya Refugee camps situated within the Teknaf and Ukhiya sub-districts, bordered by the Bandarban district to the north, Rakhine State to the east, and the Bay of Bengal to the south-southwest (Figure 1). Geographically, its coordinates span from approximately 92.114,20.913 x 92.279,21.227 20°45011.1500N to 21°17027.5100N latitude and 92°20015.8300E to 92°6038.4900E longitude. This area exhibits a varied topography, including rolling hills, plains at the foothills, and tidal floodplains (Ahammad et al., 2022). Approximately one million refugees currently reside within the 30 sq-km expanse of the Rohingya camps, rendering it one of the most densely populated regions globally. The climatic conditions in Cox's Bazar district, where the Rohingya refugee camps are located, maintain a minimum and maximum temperature ranging from around 10.82°C to 34.83°C (Rahman et al., 2015).

The settlements are divided into 33 camps, among them 7 are in the Noyapara expansion site in the Teknaf and the remaining 26 are in the Kutupalong Balukhali expansion site in Ukhiya upazila (Table 1). The density of the population of the camps varied from 1200 to 8000/sq-km in these camps (UNHCR, 2023b). With this severe density, the shelters are made with the highest flame-able materials like Bamboo, Tarpaulin, and plastic rope. Besides this structural vulnerability, the cooking practices within the Rohingya camps rely on in-house facilities, further amplifying the fire risk.

IDRiM (2025) 15 (2) **ISSN: 2185-8322**
DOI10.5595/001c.144969

Annex IV

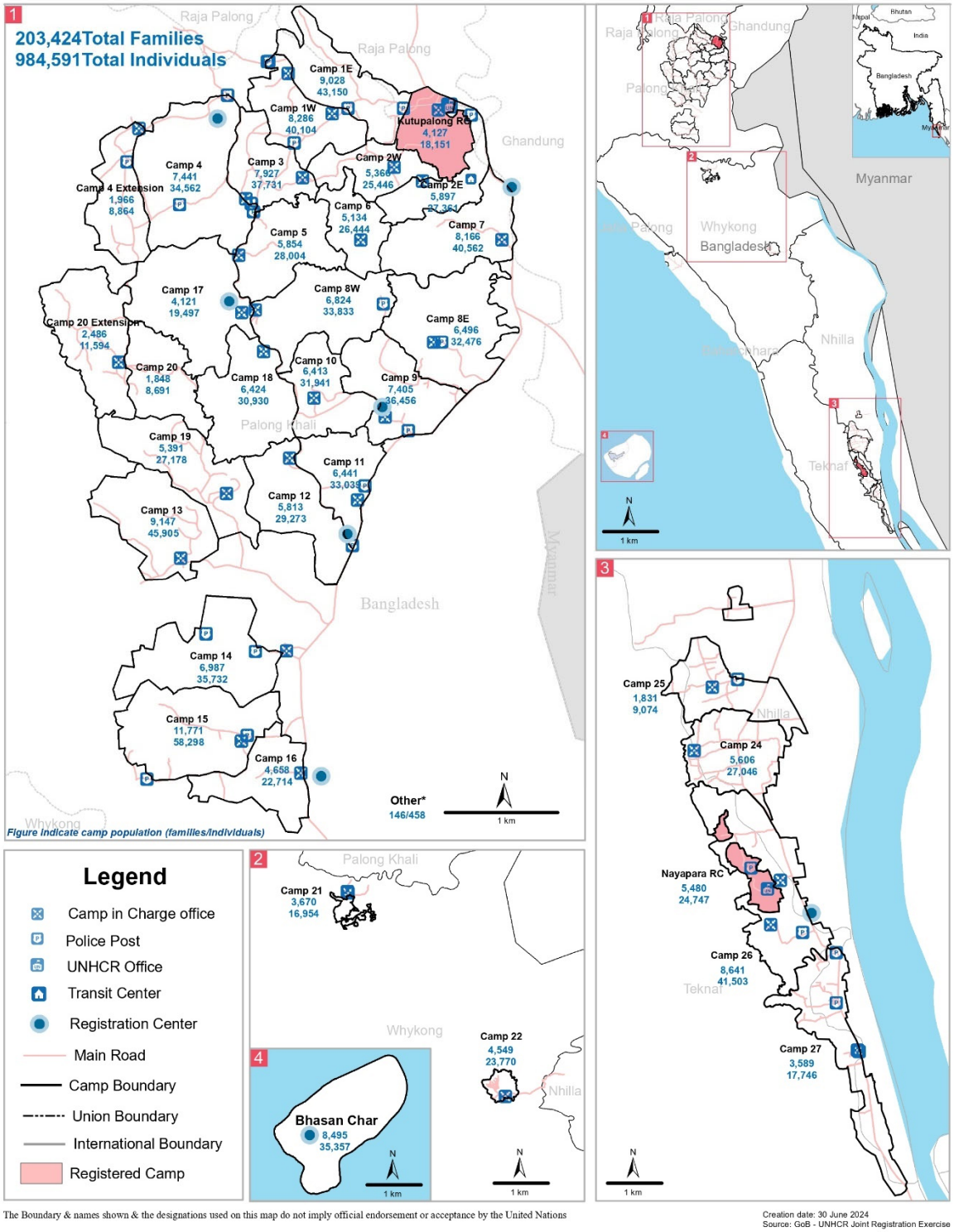

Figure 1. GoB UNHCR Camp Population and Density Map - June 2024 (UNHCR, 2024b)

3. DATA AND METHODOLOGY

3.1 Data Collection and Source of Data

The evaluation of the fire hazard risk index within the context of vulnerable communities, such as refugee settlements, necessitates a comprehensive range of data inputs. The dataset utilized in this research encompasses multiple dimensions, including settlement footprint, land surface temperature, normalized difference vegetation index, population density, and socioeconomic information pertinent to the refugee populace. The execution of this fire hazard risk assessment entails the amalgamation of a diverse array of data sources, encompassing remote sensing data as well as socio-economic and demographic insights. It is noteworthy, however, that the collection of data within refugee settlements is encumbered by several challenges.

Specifics regarding the methods and origins of data collection are given in Table 2. The data acquisition strategies for this study have been conceived as a fusion of remote sensing methodologies and supplementary references. All datasets used in this study are further visualized in Figure 2. Remote sensing data, land surface temperature (LST), Normalized Difference and Vegetation Index (NDVI); have been collected through the analysis of remote sensing datasets and Aspect and Slop have been collected from the analysis of the. Meanwhile, sources of secondary information, including governmental records, UNHCR reports, and other pertinent reports and research. Additionally, the settlement footprint, road network, and population data are the HUMANITARIAN DATA EXCHANGE (OCHA, 2023). The population data, instrumental in this study, was acquired from the collaborative UNHCR-GoB joint assessment (UNHCR, 2023b). Essential data encompassing fire-fighting vehicles, personnel trained in firefighting, and the composition of shelter-building materials were respectively extracted from the UNHCT report (Siegfried, 2022).

Table 1. Camps are in the basin of response with their administrative location, total pollution, and number of shelters footprint

Basin of Response	Camp Name	Administrative Location	Total Refugee Population	Shelter Footprint (>5 m^2)
Kutupalong and Balukhali Expansion	KTPRC, 1E, 1W, 2E, 2W, 3, 4, 4Ex, 5, 6, 7, 8E, 8W, 9, 10, 11, 12, 13, 14, 15, 16, 17, 18, 19, 20, 20Ex, 21	Palangkhali union of Ukhiya Upazila and Whykhang union of Teknaf Upazila	789,291	145,640
Unchiprang	22	Whykhang union of Teknaf Upazila	23,358	4332
Noyapara and Leda expansion	24, 25, 26, 27 and NRC	Nihla union of Teknaf Upazila	109,684	24,362

 ISSN: 2185-8322

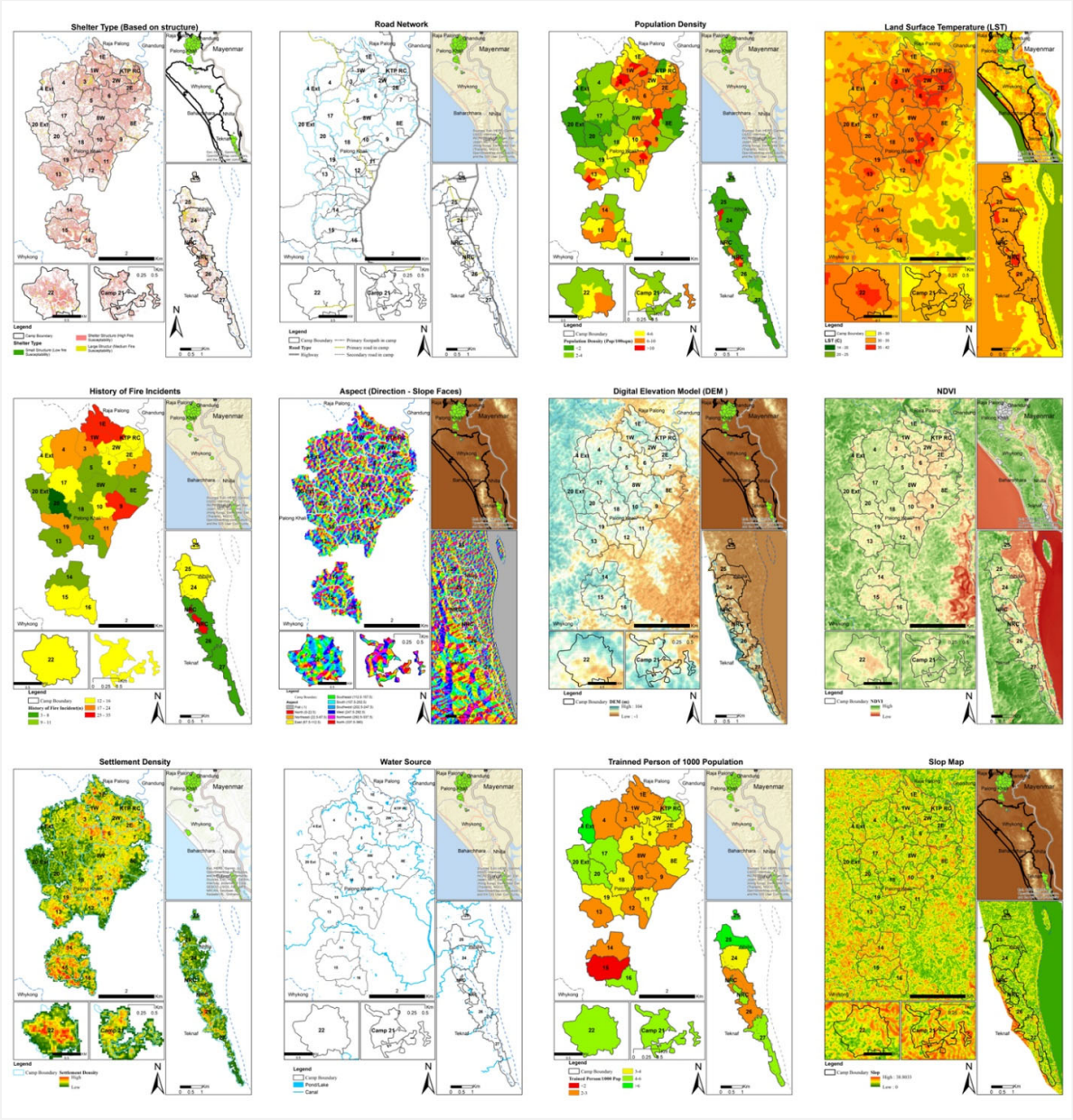

Figure 2. Available spatial data layers for multi-hazard risk assessment in Rohingya Refugee Camps, Bangladesh

3.2 Methodology

There has not been any rigorous methodology for assessing the fire risk of an informal community like Rohingya Refugees. An indicator-based blended approach has been applied for the study including the Analytical Hierarchy Process (AHP) to prioritize the indicator and an established INFORM model is used for the hazards, vulnerabilities, and risk calculation. Therefore, our research aimed to assess the susceptibility to fire at the Rohingya Refugee camp and Copping Capacity, Exposure, Vulnerability, and Risk. Consistent with this objective, we attempted to: (i) remote sensing analysis for land surface temperature (LST), NDVI, and Water source, (ii) develop an AHP for weighting the indicator and (iii) create a risk index for individuals' settlements sub-block, block, and camp in GIS interface as geospatial format.

Table 2. Details of the data products used in the present study

Parameter	Product	Source
NDVI	Satellite Image (Landsat 8 (OLI), date of acquisition 2019/02/01), UTM zone 46	https://glovis.usgs.gov/
LST		
Elevation	ALOS PALSAR – Radiometric Terrain Correction (RTC)	https://search.earthdata.nasa.gov/search/
Slop	Extract from DEM	
Aspect	Extract from DEM	
Distance from Road	Road network database of Rohingya Refugee camp. Updated: 14 February 2019	https://data.humdata.org/dataset/cox-s-bazar-existing-and-planned-access-road-network-of-all-rohingya-refugee-camps
Water Source	Water sources are extracted from the analyzed satellite image database (NDWI)	https://glovis.usgs.gov/
Shelter footprint and settlement density	HUMANITARIAN DATA EXCHANGE v1.72.3 PY3 at OCHA platform and density data extract from shelter footprint	https://data.humdata.org/dataset/bangladesh-refugee-camp-structure-footprint-march-2020
Population Density	Number of people live in one sqm area, camp-wise total population data collected from UNHCR-GoB joint assessment	https://data.unhcr.org/en/country/bgd
History of fire	NPM Daily Incidents Yearly Report 2022	https://reliefweb.int/report/bangladesh/npm-smsd-daily-incidents-yearly-report-2022
Shelter building material /Shelter Type	Structural information about the shelters such as building materials and available sources of fire at the camp	https://data.humdata.org/dataset/bangladesh-refugee-camp-structure-footprint-march-2020
Number of Trained personal for Fire fighting in 1000 people	UNHCR report	www.unhcr.org/news/stories/rohingya-refugees-lead-response-fire-threat-bangladesh-camps
Camp and Block Boundary		https://data.humdata.org/dataset/outline-of-camps-sites-of-rohingya-refugees-in-cox-s-bazar-bangladesh/resource/7cec91fb-d0a8-4781-9f8d-9b69772ef2fd

The Sentinel-2 satellite mission offers a substantial amount of high-resolution multispectral and thermal data that can be utilized to monitor changes in land surface temperature (LST). Among the two common methods widely used for LST calculation from the Sentinel-2 image's thermal band in QGIS, the Single-Channel Method was employed in this study. This method is based on the relationship between the radiance at a specific wavelength and the LST and assumes the atmospheric effect to be negligible and that the surface emissivity is known. The

formula used in this method is TIRS band digital numbers (DN) have been converted to spectral radiance using the following (1) (Sánchez et al., 2020):

$$L_\lambda = M_L \times Q_{Cal} + A_L \quad (1)$$

Where s the spectral radiance expressed in W/ (m2 ·sr·µm); M_L is 3,342× 10–4 W/ (m2 ·sr·µm) indicated in the Landsat metadata file; Q_{Cal} is the digital value (DN) of the bands that vary in a range from 0 to 255 and A_L is a dimensionless rescaling value located in the image file.

Next, to obtain the brightness temperature (T) in º Centigrade, the spectral radiance has been converted. This is the actual temperature recorded by the satellite with the precondition that the emissivity value is one, expressed as follows, Equation (2) (Sánchez et al., 2020):

$$T = \frac{K_2}{\log\left(\frac{K_1}{L_\lambda} + 1\right)} - 273.15 \quad (2)$$

Where, Landsat 8: K_1=774.8853 and K_2=1321.0789 and L_λ is the spectral radiance derived from (1).

In the present study, the ε correction based on the NDVI determination method was performed using Equation (3) (Sánchez et al., 2020) follows:

$$\varepsilon = 0.986 + 0.004 \times Pv \quad (3)$$

Where, Pv is obtained from NDVI Equation (5).

NDVI calculation Equation:

$$NDVI = \frac{NIR - Red}{NIR + Red} \quad (4)$$

To calculate the PV according to Equation (5) (Sánchez et al., 2020) . It is necessary to take the results of Equation (4) as follows:

$$Pv = \left[\frac{NDVI - NDVI_{min}}{NDVI_{max} + NDVI_{min}}\right]^2 \quad (5)$$

Where NDVI has been obtained from Equation. (4) and $NDVI_{max}$ are the maximum values of the NDVI and $NDVI_{min}$ are the minimum values of the NDVI.

LST was estimated using ε values derived from Equation (3) and using Equation (4) (Weng et al., 2004). Equation (7) is used to determine the coefficient C2 as follows:

$$LST = \frac{T}{(1 - \left(\lambda \frac{T}{C_2}\right) x log(\varepsilon))} \quad (6)$$

$$C_2 = \frac{hxc}{s} \quad (7)$$

Where LST is the Land Surface Temperature, T is the Brightness temperature of the Landsat, λ is the wavelength of the emitted radiation (Landsat 8: λ =10.8 μm and Landsat 5 and 7: λ = 11.457 μm), ε is the emissivity of the ground, h is Planck's constant with value 6.626 × 10–34 J s, c is the speed of light with value 2.998 × 108 m/s and s is Boltzmann's constant with value 1.38 × 10–23 J/K (Sánchez et al., 2020).

In QGIS, the nearest hub methodology is commonly used for distance calculations between points in different layers. This involves using the "Distance matrix" tool and selecting "Nearest (hub)" to measure distances between two shapefiles applied for the calculation of the distance from road and water source.

We collected population density data for the Rohingya refugees from the UNHCR-GoB database, measured in people per square meter. The data was transformed into a geospatial format, with area calculations from shapefiles integrated with the tabular data to determine population density in QGIS. Our secondary data source identified two types of structures in the Rohingya Refugee community: shelters used for housing and service centers for agencies. Structures smaller than 5m², like toilets, were excluded. Shelters (5-50m²) are typically made from flammable materials like bamboo and tarpaulin, while service centers (over 50m²) are built with less flammable materials like brick and metal.

The elevation data for this study was acquired from the ALOS PALSAR 12.5-meter resolution Digital Elevation Model (DEM) via the Earth Data platform. The terrain-corrected DEM data serves as the basis for calculating both slope and aspect, which are crucial parameters in understanding fire behavior.

The slope represents the rate of elevation change and can be calculated using the partial derivatives of the DEM. Aspect describes the direction a slope faces, and it influences factors like sunlight exposure and dryness, which affect fire susceptibility. For a cell in the DEM grid, the slope (in degrees) is calculated using the equation and aspect in the equation.

$$Slope = arctan\left(\sqrt{\left(\frac{\partial z}{\partial x}\right)^2 + \left(\frac{\partial z}{\partial y}\right)^2}\right) X \frac{180}{\pi} \quad (8)$$

$$Aspect = 180 + \left(\frac{180}{\pi} X\, arctan\left(\frac{\frac{\partial z}{\partial x}^2}{-\frac{\partial z}{\partial y}^2}\right)\right) \quad (9)$$

Where:

$\frac{\partial z}{\partial x}$ and $\frac{\partial z}{\partial y}$ are the rates of elevation change in the x (horizontal) and y (vertical) directions and are the rates of elevation change in the x (horizontal) and y (vertical) directions, respectively.

The aspect result is given in degrees, representing the azimuth direction (0° to 360°) of the slope. In fire assessment, areas facing south or west, which generally receive more sunlight, may exhibit higher fire risks.

Using QGIS, slope and aspect were derived from the DEM to assess factors influencing fire spread and intensity. Steeper slopes can accelerate fire propagation due to the "chimney effect," while south-facing slopes receive more sunlight, increase dryness, and increase fire susceptibility. The Raster Terrain Analysis tool was used to calculate slope and aspect, ensuring consistent processing and reproducibility of these topographical influences on fire dynamics.

To assess firefighting capacity, we used the ratio of firefighting vehicles and trained personnel per 10,000 people. Each camp operates with 100 volunteers specializing in emergency response, with support from UNHCR and IOM. Every camp is equipped with two mobile firefighting three-wheelers, operated by these volunteers.

Finally, Re-scaling normalizes indicators to have an identical range of 0.0-1 with the notion that higher is worse. The normalized indicators have been rounded to the first decimal place. The outlier often impacts the upper and lower bound of the normalization equation and affects the risk level. Therefore, the datasets go through the outlier treatment process and then normalize the equation employed. There are many techniques to identify outliers, but in line with the INFORM index interquintail ranges (IQR) technique has been used.

$$x_{i,norm} = \frac{x_i - x_{i,min}}{x_{i,max} - x_{i,min}} \times 10 \quad (10)$$

x_i $-data\ point\ for\ the\ i{-}th\ indicator's\ dataset$

$x_{i,min}$ $-minvalue\ for\ i{-}th\ indicator's\ dataset$

$x_{i,max}$ $-maxvalue\ for\ i{-}th\ indicator's\ dataset$

$x_{i,norm}$ $-\ normalized\ data\ point\ og\ the\ i{-}th\ indicator's\ dataset$

AHP for Weight Calculation

The Analytic Hierarchy Process (AHP), developed by Thomas Saaty, is a widely used mathematical technique for addressing complex decision problems with multiple criteria (Saaty, 1977, 1980). It enables decision-makers to establish priorities and make informed choices by breaking down complex decisions into a series of pairwise comparisons. AHP's key strengths include its adaptability, intuitive appeal, and ability to identify inconsistencies in evaluations, helping to reduce biases in the decision-making process (Ramanathan, 2001). However, a drawback of AHP is its reliance on subjective inputs, which can vary among experts, potentially affecting the consistency of the decisions (Kayastha et al., 2013). The relative importance between two parameters is determined through a standardized preference scale, as presented in Table 3 (Chhetri & Kayastha, 2015).

Table 3. The scale of preference between two parameters in the Analytic Hierarchy Process (AHP)

Preference Factor	Degree of Preference	Explanation
1	Equally	Two factors contribute equally to the objective
3	Moderately	Experience and judgment slightly to moderately favor one factor over another
5	Strongly	Experience and judgment strongly or essentially favor one factor over another
7	Very Strongly	A factor is strongly favored over another, and its dominance is shown in practice
9	Extremely	The evidence of favoring one factor over another is the highest degree possible of an affirmation
2,4,6,8	Intermediate	Used to represent compromises between the preferences in weights
1, 3, 5, 7 and 9	Reciprocals	Opposites Used for inverse comparison

AHP has found extensive applications in diverse fields related to environmental management and disaster risk assessment. These applications include creating risk maps for wildfires (Johnson & Christopherson, 2005) forest fires (Lamat et al., 2021; Vadrevu et al., 2010), and urban fires (Chaudhary et al., 2016; Yin et al., 2019). It has also been utilized for landslide susceptibility mapping (Semlali et al., 2019; Shahabi & Hashim, 2015), as well as aiding in the selection of landfill sites (Hashemi et al., 2017; Huang et al., 2018) and land use patterns (Kumar et al., 2021).

Saaty (1980, 1990) proposed a systematic approach known as Analytic Hierarchy Process (AHP) with the following steps:

1. Define the problem and establish its objective.
2. Create a hierarchical structure starting from the top, representing the decision maker's objectives, followed by intermediate levels comprising the criteria on which subsequent levels depend, and finally reaching the lowest level containing a list of alternatives.
3. Develop a set of pair-wise comparison matrices (of size n × n) for each lower level, with one matrix for each element from the level immediately above. These comparisons are made using a relative scale measurement, as depicted in Table 3, where each element's dominance over the others is assessed.
4. In step 3, there will be a need for n (n − 1) judgments to build the set of matrices. Reciprocals are automatically assigned in each pair-wise comparison to ensure consistency.
5. Compute the normalized principal eigenvectors, maximum eigenvalue, consistency index, and consistency ratio for each criterion.
6. Perform steps 3–5 for all levels in the hierarchy.
7. Integrate weight values (normalized principal eigenvectors) to reach an optimum decision.

The consistency is determined by using the maximum Eigenvalue (λ_{max}) to calculate the consistency index (CI) as given in Equation (11).

$$CI = \frac{\lambda_{max} - n}{n-1} \quad (11)$$

Where n is the size of the matrix.

Judgment consistency can be checked by taking the consistency ratio (CR) of CI with the appropriate value of the random consistency index (RI) given in Table 4 (Brunelli et al., 2013). If CR does not exceed 0.10, then the comparison matrix is consistent. If CR is greater than **0.1,** the comparison matrix is inconsistent. If inconsistencies in the decision process exist, the process should be repeated until a consensus is reached.

Table 4. Random Consistency Index (RI) values for different matrix sizes (n)

n	1	2	3	4	5	6	7	8	9	10	11	12	13	14	15
RI	0	0	0.58	0.90	1.12	1.24	1.32	1.41	1.45	1.49	1.51	1.53	1.56	1.57	1.59

Application of AHP in Fire Potential Mapping

In this study, a comprehensive comparative analysis was performed using a quantitative scale from 1 to 9 for direct relationships and from 1/2 to 1/9 for inverse relationships. Elements were systematically compared in pairs across hierarchical tiers based on their relative significance. Pairwise comparison matrices were constructed starting from the top tier, ensuring positive matrix values throughout thereby facilitating the derivation of relative weights for each criterion (Gong et al., 2023; Wang et al., 2021)

To assess each causative factor class, a questionnaire was distributed to eight experts from the fields of geology, disaster management, engineering, emergency response and preparedness personal. The averaged relative weight values, calculated from their responses, are presented in Table 5.

$$A = [a_{ij}] = \begin{bmatrix} a_{11} & a_{12} & \dots & a_{1n} \\ a_{21} & a_{22} & \dots & a_{2n} \\ \dots & \dots & \dots & \dots \\ a_{n1} & a_{n2} & \dots & a_{nn} \end{bmatrix} \quad (12)$$

Such that $a_{ij} > 0$.

Table 5 presents the normalized principal eigenvector calculated for indicators like population density, settlement density, building materials, slope factor, aspect, and DEM under the Vulnerability category, along with LST, NDVI, and historical fire events under Hazard Exposure, and the number of trained personnel, road network, and water sources under Capacity. These factors contribute to assessing fire potential zones. The table also displays the consistency test results for each criterion, with Consistency Ratios (CR) for categories like population density, LST, and personnel training all under 0.10, confirming that the ratings for these indicators are consistent.

Table 5. Indicators and weight of the indicator based on the AHP frameworks

Category	Indicator	Weight	Lambda Max	C.I	C.R
Vulnerability	Population density	0.19	6.47	0.094	0.076
	Settlement density	0.23			
	Building Materials	0.36			
	Slop Factor	0.08			
	Aspect	0.1			
	DEM	0.06			
Hazard Exposure	LST	0.41	3.029	0.015	0.025
	NDVI	0.11			
	History	0.48			
Capacity	Number of trained Personal	0.63	3.038	0.019	0.033
	Road Network	0.26			
	Water Source	0.11			

3.3 Risk Calculation

When employing the Analytic Hierarchy Process (AHP) for deriving the weights of each criterion, we computed the risks associated with each shelter within the camp. The risk calculation was based on three parameters: hazard/hazard exposure, vulnerability of the elements, and capacity. Our approach utilized a simple formula where risk is the product of hazard and vulnerability, inversely scaled by capacity. The weight calculation ensured a total criterion weight of 1, equivalent to 100%, thereby resulting in a risk level spanning from 0 to 1. Within this study, we selected 12 criteria, considering data availability and data accessibility. Among these criteria, we focused on four indicators—LST, NDVI, SF, and HF—for exposure analysis (Equation (13)). Additionally, NTP and NFFV were employed for capacity assessment (Equation (15)). For vulnerability assessment (Equation (14)), we chose six criteria: water source, road accessibility, population density, settlement density, DEM, and shelter construction materials. The risk of individual shelters/structures was evaluated based on the outcomes of their respective hazard, vulnerability, and capacity factors.

$$HE = (LST \times 0.41) + (NDVI * 0.11) + (HF \times 0.48) \quad (13)$$

$$V = (\mathrm{PD} \times 0.19) + (\mathrm{SD} \times 0.23) + (\mathrm{SBM} \times 0.36) + (\mathrm{Aspect} \times 0.10) + (\mathrm{Slop} \times 0.08) + (\mathrm{DEM} \times 0.06) \quad (14)$$

$$C = (NTP \times 0.36) + (RN \times 0.26) + (WN \times 0.11) \quad (15)$$

$$R = \sum_{i=1}^{n} (HE_i \times w_i) + (V_i \times w_i) + (C_i \times w_i) \quad (16)$$

The final risk score has been normalized and ranges from 0 to 10 where 0 means the lowest value of risk but it does not mean that there has not been any risk and 10 means the highest level of risk but does not mean the complete risk. For better perception and understanding, the settlements have been shortened into five categories. In this study, we use the risk threshold used by the modification INFORM risk index methodology (UNDRR, 2022b.) In the INFORM index, the risk value categorized based on risk ranges from 0 to 10 given in Table 6.

Table 6. Fixed thresholds at the level of dimensions of the risk of the structure due to fire hazards at the Rohingya refugee camp

Risk Category	INFORM Range	The range for this Study
Very high	>= 6.5	>= 6.5
High	5.0 to 6.4	5.0 to 6.4
Medium	3.5 to 4.9	3.5 to 4.9
Low	2.0 to 3.4	2.0 to 3.4
Very Low	<= 1.9	<= 1.9

Eminently, the lowest stratum of risk is denoted as the 'very low-risk category, encompassing individuals exhibiting risk scores that span from zero to 0.3. Conversely, the apex of the risk continuum is characterized by the 'very high-risk' category, encompassing those with risk scores surpassing the threshold of 0.6. The 'medium risk' category occupies a span ranging from 0.4 to 0.5, while the 'high risk' designation encapsulates scores between 0.5 and 0.6. Concluding the taxonomy, the 'low risk' category encompasses values oscillating within the range of 0.3 to 0.4.

4. RESULT

This is evident that fire in the IS does not follow any pattern. Thus, it is very difficult to assess and index the fire risk of a refugee camp settled in vulnerable areas. However, GIS-based hybrid approaches help us to develop risk indexing for fire hazards using available datasets. In the analysis, firstly we get weight from the AHP framework, and then GIS analysis has been performed to extract values. Then, using the values, Hazard Exposure (HE), Vulnerability, and Capacity have been assessed and finally, risk value/index has been calculated and categorized based on the INFORM methodology.

4.1 Exposure

Based on previous studies and the available data, fire hazard exposure in the camps has been assessed using three key indicators: Land Surface Temperature (LST), Normalized Difference Vegetation Index (NDVI), and historical records of fire incidents. These indicators help paint a broad picture of fire risks at the camp level, though they are more focused on macro-level patterns rather than pinpointing risks at the individual shelter level. Figure 3(c) illustrates the distribution of hazard exposure among households, categorizing them into five distinct groups: Very High, High, Moderate, Low, and Very Low.

ISSN: 2185-8322
DOI10.5595/001c.144969

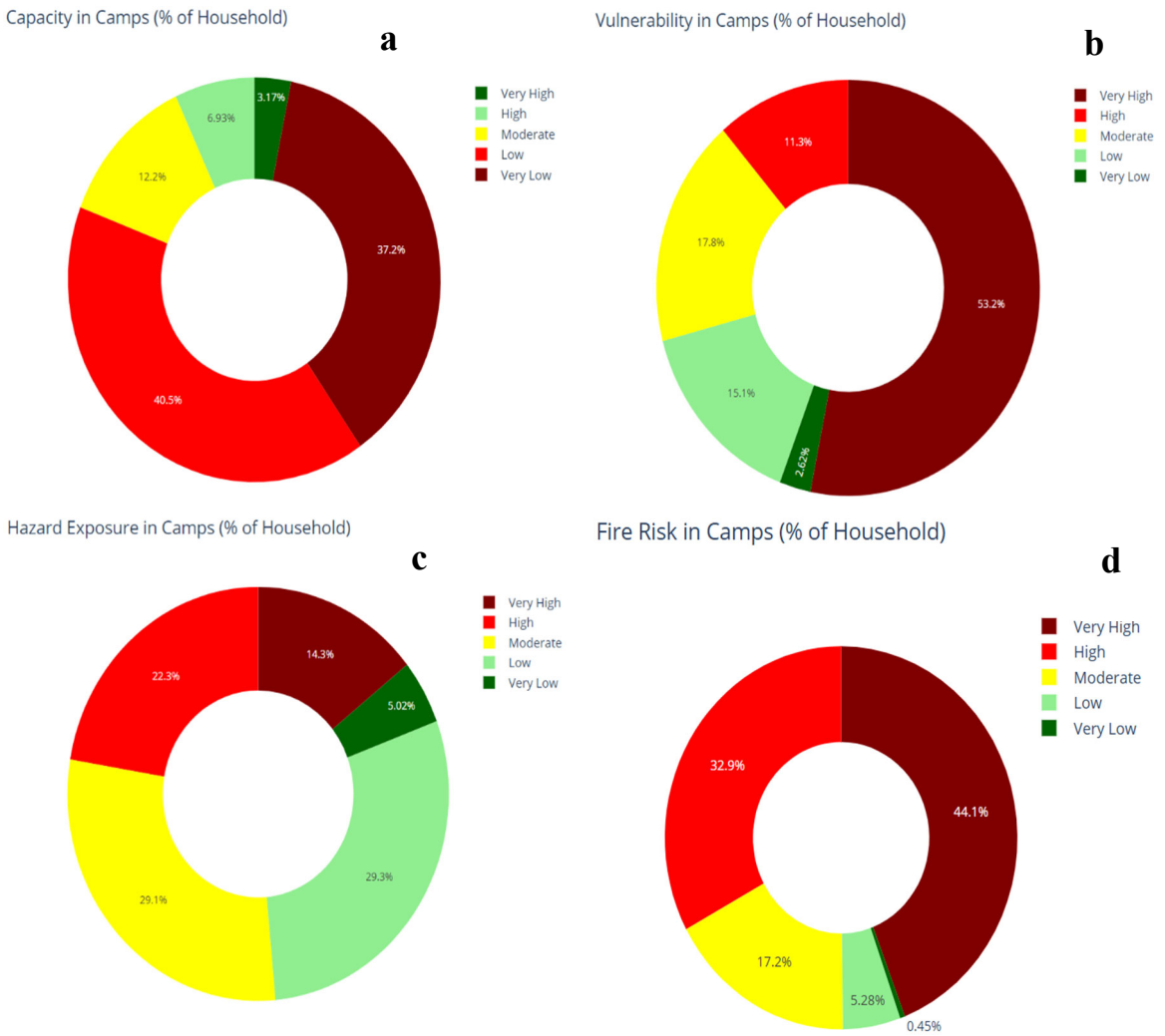

Figure 3. Overall fire (a) capacity, (b) vulnerability, (c) exposure and (d) risk of the camp settlements

The analysis shows that a majority of households fall into the Low and Moderate exposure categories, which together comprise around 58.4% of the shelters. This indicates that more than half of the population is at relatively lower exposure to fire hazards. However, a notable proportion of households are more vulnerable, with 22.3% of households classified as being in the High exposure group and 14.3% in the Very High exposure group. These households are at a significantly elevated risk of fire, potentially due to factors such as localized high temperatures, vegetation density, and past fire incidents in their proximity. Only a small fraction, 5.02% of households, is categorized as having Very Low exposure to fire hazards.

While this exposure assessment provides valuable insights, it does have limitations. The analysis relies heavily on macro-level indicators like LST and historical fire incidents at the camp level, which may not fully capture the specific vulnerabilities of individual shelters. However, this approach does offer a comparative understanding of fire risk across the camps, enabling better-informed decisions for fire hazard mitigation and disaster preparedness efforts.

4.2 Vulnerability

In risk analysis, vulnerability assessment is essential for prioritizing areas in need of intervention, particularly in high-risk informal settlements such as Rohingya refugee camps. This study examines fire hazard vulnerability by analyzing six key indicators, with an overall vulnerability score calculated using the AHP and illustrated in Figure 3(b). Overall findings reveal in a detailed breakdown that most of the shelters are in the very high and highly vulnerable categories combined with 64.5% of the shelters 53.2% and 11.3% are very high and high vulnerable categories respectively. However, the rest of the shelters lie in the moderate 17.8%, low 15.1%, and very low 2.62% respectively.

However, the overall results do not represent the actual scenario of the vulnerability distribution in the camp settlement the individual camp and shelter level vulnerability may provide a better understanding of the vulnerability. However, in this study, we covered the individual shelter-level vulnerability camp camp-level vulnerability given in the additional data.

4.3 Capacity

Capacity serves as a critical measure of community resilience, reflecting how well a community can respond to and recover from incidents. In informal settlements, especially those exposed to fire hazards, socioeconomic and administrative resources to respond effectively are often limited. In the Rohingya refugee camps, however, there have been coordinated efforts to strengthen fire preparedness and response capacity, providing some resilience against fire hazards.

In this study, capacity indicators—such as preparedness level, community response mechanisms, and resource availability—were assessed and are illustrated in Figure 3(a). The results reveal that most households fall into the lower capacity categories. Specifically, 37.2% of households are in the very low-capacity category, shown in dark red, while 40.5% fall into the low-capacity category, marked in bright red. This leaves a minority of households in the moderate (12.2%) and high (6.93%) capacity categories, with only 3.17% in the very high-capacity range, depicted in green. This distribution highlights significant capacity limitations within the camps, with nearly 78% of households in low or very low-capacity categories.

4.4 Fire Risk and Risk Index

The risk is the function of the hazard exposure, vulnerability and capacity, and overall fire hazard risk of the camp settlements illustrated in Figure 3(d). The objective of this study is the shelter-level risk index, and this overall representation is the summary of the individual shelter risk index. The analysis highlights that a significant proportion of households, approximately 44.1%, are categorized under the "Very High" risk level. This finding underscores the severe fire risk faced by nearly half of the camp population, indicating an urgent need for focused fire prevention and response interventions. The "High" risk category accounts for 32.9% of households, further emphasizing the heightened vulnerability in these settings.

Moderate risk is associated with 17.2% of households, suggesting that these households also face notable but relatively less critical fire risks. Only a small percentage of households, 5.28%, and 0.45% fall under the "low" and "very low" risk categories, respectively, indicating that few areas exhibit minimal fire risk.

However detailed risk index data has been given in the supplementary data the camp level risk is illustrated in Figure 4. These graphs categorize the fire risk for households within the camps into five distinct levels: very high, high, moderate, low, and very low and the overall distribution of risk across the camps reveals significant variations in fire hazard risk.

Several camps are overwhelmingly categorized as very high risk. For instance, camp 1E has 86.3% of households in the very high-risk group, while Camp 1W has 89%. Similar patterns are observed in Camp 9, where 87.7% of households are also categorized as very high risk. These camps demonstrate a clear concentration of fire hazards, possibly due to a combination of factors such as dense living conditions, high temperatures, and historical fire incidents. Other camps, such as Camp 5 and Camp 2E, also have high proportions of very high risk, with 52.6% and 62.5% of households, respectively, in this category. This underscores the significant fire risk faced by households in these areas.

On the other hand, some camps have a mid-level of risk. For example, Camp 4 Ex and Camp 20 Ex show a considerable proportion of households in the low and very low-risk categories, suggesting relatively lower fire risk in these locations. In Camp 4 Ex, 33.1% of households fall under the Moderate risk group, while 41.4% are categorized as low and 16.5% as very low. Similarly, Camp 20 Ex has 41.5% of households in the low-risk group, and 28.6% in the moderate group.

Camp 12, for instance, has 45.4% of households facing moderate risk, while 28.5% are in the High-risk category and 9.82% are in the very high category. This distribution highlights the variability of fire hazards within the camp, with some households being more exposed than others. Camp 25 also shows a significant proportion of households in the low-risk category (42.5%), with a smaller number facing high and very high risks (8.67% and 0.59%, respectively). This camp represents a more favorable fire hazard scenario compared to others.

A few camps, such as Camp 17 and Camp 3, have notable portions of households in the high and moderate risk categories, suggesting a mid-level fire risk that is neither overwhelmingly high nor low. In Camp 17, 65.7% of households are in the high-risk group, while 19.8% are in moderate, and only 14.5% fall into the Low category. Similarly, Camp 3 has 72.3% of households facing very high risk, while 25.7% are in high risk, indicating a predominantly high-risk situation.

5. DISCUSSION AND CONCLUSION

The Fire Hazard Risk Index (FHRI) developed in this study serves as a crucial tool for identifying and assessing the fire risks and decision-making support for better servicing the

vulnerable community. By leveraging the AHP, we systematically weighted the importance of 12 criteria that contribute to fire hazards. Although the complexity of defining these criteria and assigning pairwise weights poses challenges, expert judgment and literature-based insights helped mitigate this issue.

Figure 4. Camp-wise fire risk index (% of shelter in Risk)

The results from this analysis highlight those certain camps, such as Camps 1E, 1W, 9, 10, 11, and 15 are situated in the highest fire risk-prone areas within the Ukhiya basin and Camp NRC in the Teknaf sub-basin. Approximately 44.1% of households face a "Very High" fire risk, highlighting the urgent need for targeted prevention and response measures, while 32.9% are categorized as "High" risk, indicating significant vulnerability. Only 17.2% are at "Moderate" risk, with minimal percentages falling into the "Low" (5.28%) and "Very Low" (0.45%) categories. This spatial distribution of fire risk aligns with historical fire patterns, which often concentrate in highly populated and resource-constrained sections of the camps.

Incorporating 12 distinct factors for evaluating fire hazard risk, our analysis highlights the elevated risk levels across the camp's shelters and substantiates previous observations on fire patterns within refugee settlements. By understanding the specific areas and structures at high risk, camp management can target fire prevention resources more effectively, prioritizing high-risk shelters and investing in community-based fire response training. However, the capacity limitations observed in the camps—particularly the lack of adequate resources and emergency response mechanisms—pose additional challenges. This indicates the need for both immediate risk mitigation strategies and long-term capacity-building programs to enhance resilience.

The FHRI model presented in this study provides a comprehensive and structured approach to fire hazard assessment within the Rohingya refugee camps. By utilizing a combination of GIS-based data analysis, AHP weighting, and the INFORM methodology for risk categorization, we have generated a detailed risk index that identifies high-risk shelters and camp zones. This risk indexing enables a more informed decision-making process for stakeholders involved in fire prevention, preparedness, and response efforts.

This study underscores the necessity of sustainable fire risk management strategies tailored to the camp environment. A well-informed approach to capital investment and resource allocation will be pivotal in addressing the fire hazard risks within these settlements. Future work could refine the risk assessment further by incorporating additional factors, such as real-time climatic data or community-level socio-economic indicators, which would enhance the accuracy and relevance of the risk assessments. Ultimately, the FHRI model has the potential to guide practical, targeted, and effective fire risk reduction measures, ensuring greater safety and resilience for this vulnerable refugee population.

REFERENCES

Ahammad, R., Stacey, N., Sunderland, T., & Sangha, K. K. (2022). Land Use Preference for Ecosystem Services and Well-Being in Chittagong Hill Tracts of Bangladesh. *Forests 2022, Vol. 13, Page 2086*, *13*(12), 2086. https://doi.org/10.3390/F13122086

Brunelli, M., Critch, A., & Fedrizzi, M. (2013). A note on the proportionality between some consistency indices in the AHP. *Applied Mathematics and Computation*, *219*(14), 7901–7906. https://doi.org/10.1016/J.AMC.2013.01.036

Chaudhary, P., Chhetri, S. K., Joshi, K. M., Shrestha, B. M., & Kayastha, P. (2016). Application of an Analytic Hierarchy Process (AHP) in the GIS interface for suitable fire

site selection: A case study from Kathmandu Metropolitan City, Nepal. *Socio-Economic Planning Sciences*, *53*. https://doi.org/10.1016/j.seps.2015.10.001

Chhetri, S. K., & Kayastha, P. (2015). Manifestation of an analytic hierarchy process (AHP) model on fire potential zonation mapping in Kathmandu metropolitan City, Nepal. *ISPRS International Journal of Geo-Information*, *4*(1). https://doi.org/10.3390/ijgi4010400

Cicione, A., Wade, C., Spearpoint, M., Gibson, L., Walls, R., & Rush, D. (2021). A preliminary investigation to develop a semi-probabilistic model of informal settlement fire spread using B-RISK. *Fire Safety Journal*, *120*, 103115. https://doi.org/10.1016/J.FIRESAF.2020.103115

Flores Quiroz, N., Walls, R., & Cicione, A. (2021). Developing a framework for fire investigations in informal settlements. *Fire Safety Journal*, *120*, 103046. https://doi.org/10.1016/J.FIRESAF.2020.103046

Flores Quiroz, N., Walls, R., Chamberlain, P., Tan, G., & Milke, J. (2023). Incident Report and Analysis of the 2021 Cox's Bazar Rohingya Refugee Camp Fire in Bangladesh. *Fire Technology*. https://doi.org/10.1007/s10694-023-01406-7

Gong, A., Huang, Z., Liu, L., Yang, Y., Ba, W., & Wang, H. (2023). Development of an Index for Forest Fire Risk Assessment Considering Hazard Factors and the Hazard-Formative Environment. *Remote Sensing*, *15*(21). https://doi.org/10.3390/rs15215077

Guevara Arce, S., Jeanneret, C., Gales, J., Antonellis, D., & Vaiciulyte, S. (2021). Human behaviour in informal settlement fires in Costa Rica. *Safety Science*, *142*, 105384. https://doi.org/10.1016/J.SSCI.2021.105384

Hashemi, M., Pourzamani, H. R., Chavoshani, A., Menglizadeh, N., Parseh, I., Heidari Farsani, M., Heidari, F., & Rezaei, S. (2017). Industrial landfill site selection using Analytical Hierarchy Process (Case study: Razi industrial town of Isfahan-Iran). *J Adv. Environ Health Res*, *5*.

Huang, Q., Huang, J., Zhan, Y., Cui, W., & Yuan, Y. (2018). Using landscape indicators and Analytic Hierarchy Process (AHP) to determine the optimum spatial scale of urban land use patterns in Wuhan, China. *Earth Science Informatics*, *11*(4). https://doi.org/10.1007/s12145-018-0348-4

Hu, J., Xie, X., Shu, X., Shen, S., Ni, X., & Zhang, L. (2022). Fire Risk Assessments of Informal Settlements Based on Fire Risk Index and Bayesian Network. *International Journal of Environmental Research and Public Health*, *19*(23), 15689. https://doi.org/10.3390/IJERPH192315689

IOM. (2023a). *Bangladesh — Camp 11 Fire Incident Situational Assessment: Rohingya Refugee Response, Cox's Bazar (June 2023) - Bangladesh | ReliefWeb*. https://reliefweb.int/report/bangladesh/bangladesh-camp-11-fire-incident-situational-assessment-rohingya-refugee-response-coxs-bazar-june-2023

IOM. (2023b, June 13). *NPM SMSD Daily Incidents Yearly Report 2022 - Bangladesh | ReliefWeb*. https://reliefweb.int/report/bangladesh/npm-smsd-daily-incidents-yearly-report-2022

Johnson, P., & Christopherson, G. (2005). Using the Analytic Hierarchy Process to Create a Wildfire Model. In *Proceedings.Esri.Com* (Vol. 1).

Kayastha, P., Dhital, M. R., & De Smedt, F. (2013). Application of the analytical hierarchy process (AHP) for landslide susceptibility mapping: A case study from the Tinau

watershed, west Nepal. *Computers and Geosciences*, *52*. https://doi.org/10.1016/j.cageo.2012.11.003

Kazerooni, Y., Gyedu, A., Burnham, G., Nwomeh, B., Charles, A., Mishra, B., Kuah, S. S., Kushner, A. L., & Stewart, B. T. (2016). Fires in refugee and displaced persons settlements: The current situation and opportunities to improve fire prevention and control. *Burns*, *42*(5), 1036–1046. https://doi.org/10.1016/j.burns.2015.11.008

Kumar, A., Vema, V. K., Kurian, C., Thomas, J., & Sudheer, K. P. (2021). A decision support system for the identification of critical zones in a watershed to implement land management practices. *Stochastic Environmental Research and Risk Assessment*, *35*(8). https://doi.org/10.1007/s00477-021-01983-5

Lamat, R., Kumar, M., Kundu, A., & Lal, D. (2021). Forest fire risk mapping using analytical hierarchy process (AHP) and earth observation datasets: a case study in the mountainous terrain of Northeast India. *SN Applied Sciences*, *3*(4). https://doi.org/10.1007/s42452-021-04391-0

MoDMR. (2021). *Bangladesh Climate and Disaster Risk Atlas*. https://doi.org/10.22617/TCS210518

Morrissey, J., & Taylor, A. (2006). Fire Risk in Informal Settlements: A South African Case Study. *Open House International*, *31*(1), 98–105. https://doi.org/10.1108/OHI-01-2006-B0012

Mukherjee, M., Abhinay, K., Rahman, M. M., Yangdhen, S., Sen, S., Adhikari, B. R., Nianthi, R., Sachdev, S., & Shaw, R. (2023). Extent and evaluation of critical infrastructure, the status of resilience and its future dimensions in South Asia. *Progress in Disaster Science*, *17*, 100275. https://doi.org/10.1016/J.PDISAS.2023.100275

OCHA. (2023). *Rohingya Refugee Crisis - Humanitarian Data Exchange*. https://data.humdata.org/event/rohingya-displacement?

Parvin, G. A., Dasgupta, R., Abedin, M. A., Sakamoto, M., Ingirige, B., Kibria, M. G., Fujita, K., Basu, M., Shaw, R., & Nakagawa, H. (2022). Disaster experiences, associated problems and lessons in southwestern coastal Bangladesh: exploring through participatory rural appraisal to enhance resilience. *Https://Doi.Org/10.1080/23789689.2022.2138165*, *8*(sup1), 223–236. https://doi.org/10.1080/23789689.2022.2138165

Quiroz, N. F., Walls, R., & Cicione, A. (2021). Towards understanding fire causes in informal settlements based on inhabitant risk perception. *Fire*, *4*(3). https://doi.org/10.3390/FIRE4030039

Rahman, A., Jiban, Md. J. H., & Munna, S. A. (2015). Regional Variation of Temperature and Rainfall in Bangladesh: Estimation of Trend. *Open Journal of Statistics*, *5*(7), 652–657. https://doi.org/10.4236/OJS.2015.57066

Ramanathan, R. (2001). A note on the use of the analytic hierarchy process for environmental impact assessment. *Journal of Environmental Management*, *63*(1). https://doi.org/10.1006/jema.2001.0455

Saaty, T. L. (1977). A scaling method for priorities in hierarchical structures. *Journal of Mathematical Psychology*, *15*(3). https://doi.org/10.1016/0022-2496(77)90033-5

Saaty, T. L. (1980). The Analytic Hierarchy Process: Planning, Priority Setting, Resource Allocation (Decision Making Series). *Mathematical Modelling*.

Saaty, T. L. (1990). How to make a decision: The analytic hierarchy process. *European Journal of Operational Research*, *48*(1). https://doi.org/10.1016/0377-2217(90)90057-I

Sánchez, J. M., Galve, J. M., González-Piqueras, J., López-Urrea, R., Niclòs, R., & Calera, A. (2020). Monitoring 10-m LST from the combination MODIS/Sentinel-2, validation in a high contrast semi-arid agroecosystem. *Remote Sensing*, *12*(9). https://doi.org/10.3390/RS12091453

Semlali, I., Ouadif, L., & Bahi, L. (2019). Landslide susceptibility mapping using the analytical hierarchy process and GIS. *Current Science*, *116*(5). https://doi.org/10.18520/cs/v116/i5/773-779

Shahabi, H., & Hashim, M. (2015). Landslide susceptibility mapping using GIS-based statistical models and Remote sensing data in tropical environment. *Scientific Reports*, *5*. https://doi.org/10.1038/srep09899

Siegfried, K. (2022). *Rohingya refugees lead response to fire threat in Bangladesh camps | UNHCR*. https://www.unhcr.org/news/stories/rohingya-refugees-lead-response-fire-threat-bangladesh-camps

UNDRR. (2022a). *Global Assessment Report on Disaster Risk Reduction 2022: Our World at Risk: Transforming Governance for a Resilient Future*. https://doi.org/10.18356/9789210015059

UNDRR. (2022b, August 25). *Bangladesh INFORM Sub-National Risk Index 2022 | UNDRR*. https://www.undrr.org/publication/bangladesh-inform-sub-national-risk-index-2022

UNHCR. (2023a). *Global Trends: Forced Displacement in 2022 - World | ReliefWeb*. https://reliefweb.int/report/world/global-trends-forced-displacement-2022?gclid=Cj0KCQjwoK2mBhDzARIsADGbjeqqnE7TDtyRr-WkGXZ5rFzJXCyf_SRLB_70NPswtWe1xzba4FFqbMoaAisMEALw_wcB

UNHCR. (2023b). *Refugee Statistics | USA for UNHCR*. https://www.unrefugees.org/refugee-facts/statistics/

UNHCR. (2024a). *Global Appeal 2024 | Global Focus*. https://reporting.unhcr.org/global-appeal-2024

UNHCR. (2024b). *Joint Government of Bangladesh - UNHCR Camp Population and density map - as of June 2024*. https://data.unhcr.org/en/documents/details/109755

Vadrevu, K. P., Eaturu, A., & Badarinath, K. V. S. (2010). Fire risk evaluation using multicriteria analysis-a case study. *Environmental Monitoring and Assessment*, *166*(1–4). https://doi.org/10.1007/s10661-009-0997-3

Wang, Y., Hou, L., Li, M., & Zheng, R. (2021). A Novel Fire Risk Assessment Approach for Large-Scale Commercial and High-Rise Buildings Based on Fuzzy Analytic Hierarchy Process (FAHP) and Coupling Revision. *International Journal of Environmental Research and Public Health Article*. https://doi.org/10.3390/ijerph18137187

Weng, Q., Lu, D., & Schubring, J. (2004). Estimation of land surface temperature-vegetation abundance relationship for urban heat island studies. *Remote Sensing of Environment*, *89*(4). https://doi.org/10.1016/j.rse.2003.11.005

Yin, C., Qi, K., Li, K., Duan, Q., Gao, L., & Sun, J. (2019). Urban Fire Risk Evaluation Based on 2-tuple AHP-Taking the 8th Division with Shihezi City for Example. *2019 9th International Conference on Fire Science and Fire Protection Engineering, ICFSFPE 2019*. https://doi.org/10.1109/ICFSFPE48751.2019.9055872